Precise Torque Control of Induction Motor with On-Line Parameter Identification in Consideration of Core Loss

Toshihiko Noguchi [1], Paiboon Nakmahachalasint [2], and Narin Watanakul [2]

[1] : Nagaoka University of Technology
1603-1 Kamitomioka, Nagaoka 940-21, JAPAN
Phone : +81-258-46-6000, Fax : +81-258-46-6506
E-mail : omom@voscc.nagaokaut.ac.jp

[2] : Thammasat University
Khlong-Luang, Pathum-Thani 12121, THAILAND
Phone : +66-2-516-4551, Fax : +66-2-516-0974
E-mail : paiboon@ipied.tu.ac.th

Abstract — **This paper describes improved torque control of an induction motor. The control is based on direct field orientation with a rotor flux simulator, and motor parameters in the simulator are estimated by a robust identifier with no sensitivity to the stator resistance. Owing to model mismatch in the controller caused by the equivalent core loss resistance, however, both the field orientation and the parameter identification cannot be carried out perfectly, which results in degradation of torque control performance. In order to improve accuracy of the output torque, the proposed system employs a modified machine model taking the core loss into consideration. Consequently, it has been verified through computer simulations that the technique achieves high precision in torque control within a few percent errors.**

I. Introduction

The principle of field-oriented control has inherently been derived on the assumption that no core loss is in the induction motor model. In recent years, some papers have reported that the core loss detrimentally affects the field orientation, especially torque control accuracy, unless the core loss are taken into consideration [1]-[3]. However, there have probably been few reports that dealt with direct field-oriented control (flux-feedback field orientation) with on-line identification of the motor parameters incorporating the core loss. In order to achieve highly precise torque control by the direct field orientation, it is substantial to comprehensively modify not only the field-oriented controller but also the parameter identifier by taking the core loss into consideration. This paper describes a quite simplified technique for improvement of torque control accuracy which is based on the above modified system, and shows possibility of reducing the output torque error down to less than a few percent through computer simulations.

II. Basic Concept of Direct Field-Oriented Control and Parameter Identification

Fig. 1 and 2 show schematic diagrams of the direct field-oriented controller and the on-linc parameter identifier respectively [4]. The direct field orientation is performed on the basis of the following equations :

$$i_{1dq}^{*} = i_{1d}^{*} + \mathrm{j} i_{1q}^{*} = G_{AFR}\left\{|\psi_2|^{*} - |\hat{\psi}_2|\right\} + \mathrm{j}\frac{L_{22}}{M}\frac{T^{*}}{|\psi_2|^{*}}, \quad (1)$$

$$\hat{\psi}_{2\alpha\beta} = \frac{\hat{M}}{1+(\mathrm{p}-\mathrm{j}\omega_m)\hat{\tau}_2} i_{1\alpha\beta}, \quad (2)$$

$$\hat{i}_{1dq} = \frac{\overline{\hat{\psi}_{2\alpha\beta}}}{|\hat{\psi}_2|} i_{1\alpha\beta} \text{ and} \quad (3)$$

$$v_{1\alpha\beta}^{*} = \frac{\hat{\psi}_{2\alpha\beta}}{|\hat{\psi}_2|} v_{1dq}^{*}, \quad (4)$$

where the motor variables and parameters are defined as follows :

i_1 : stator current vector,
v_1 : stator voltage vector,
ψ_2 : rotor flux vector,
T : output torque,
ω_m : rotor speed,
τ_2 : rotor time constant,
L_{22} : rotor inductance,
M : magnetizing inductance,
ℓ : leakage inductance,

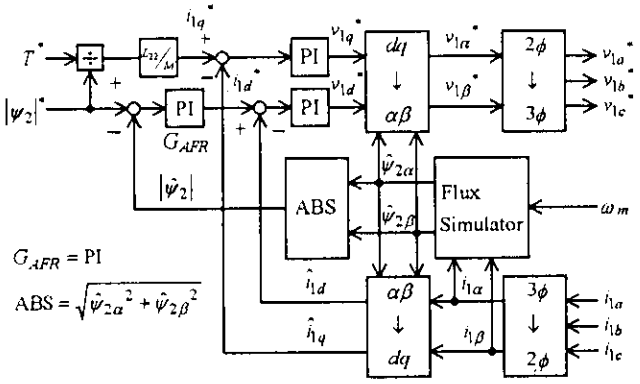

(a) Current controller.

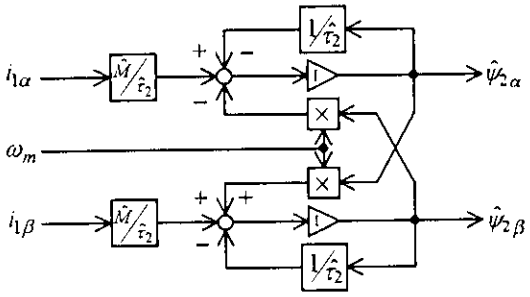

(b) Rotor flux simulator.

Fig. 1. Basic configuration of direct field-oriented controller.

G_{AFR} : transfer function (PI) of flux regulator,

p : differential operator,

j : imaginary unit,

x^* : command value of x,

$\hat{x}$: estimated value of x,

$\overline{x}$: complex conjugate of x,

$|x|$: amplitude of x,

$\alpha\beta$: vector on stator ($\alpha-\beta$) coordinates, and

dq : vector on rotor flux ($d-q$) coordinates.

The first equation is regarded as a feedforward block which determines amplitudes of the d-axis and q-axis components of the stator current command. The d-axis current command is obtained from an output of the PI controller with respect to an amplitude of the rotor flux, while the q-axis current command is directly calculated from the torque command. On the other hand, the second equation is a feedback block with respect to the rotor flux, which gives an estimated value of the flux using the motor model with the parameters in order to perform coordinate transformations described by (3) and (4).

The parameter identifier shown in Fig. 2 is based on a model reference adaptive system, which tunes the magnetizing inductance at no load and the rotor time

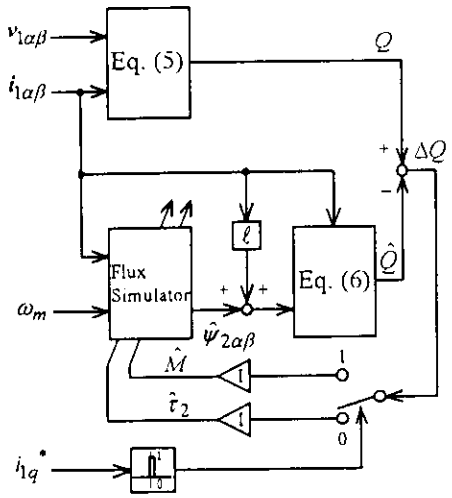

Fig. 2. Parameter identifier with robustness to stator resistance.

constant at loaded condition in the flux simulator by taking advantage of instantaneous reactive power. The instantaneous reactive power which is calculated by the following equation is used as a reference model :

$$Q = \mathrm{Im}\left(v_{1\alpha\beta}\overline{i_{1\alpha\beta}}\right). \tag{5}$$

On the other hand, the following equation gives a mathematical model of the instantaneous reactive power with respect to the estimated rotor flux and the stator current :

$$\hat{Q} = \mathrm{Im}\left(\frac{M}{L_{22}}\mathrm{p}\hat{\psi}_{2\alpha\beta}\overline{i_{1\alpha\beta}} + \ell\mathrm{p}i_{1\alpha\beta}\overline{i_{1\alpha\beta}}\right). \tag{6}$$

Since both of the above equations have no influence of the stator resistance, the configuration of Fig. 2 enables the identifier to achieve robust estimation of the motor parameters in (2) against the stator resistance. The core loss in the induction motor, however, has not been incorporated in the control and identification algorithms described above. Owing to the model mismatch caused by the core loss, both the field orientation and the parameter identification cannot be carried out perfectly, which results in degradation of torque control accuracy.

III. Equivalent Core Loss Resistance and Its Influence on Torque Control

A. Experimental Measurement of Motor Parameters

Since the core loss of the motor has been taken into consideration in neither the control nor the identification, the output torque error of not a few percent can probably remain owing to the model mismatch on the field

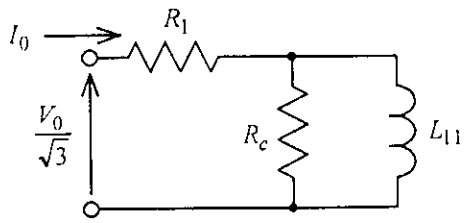

(a) Equivalent circuit at no load.

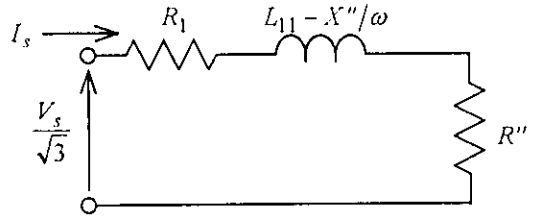

(b) Equivalent circuit with rotor locked.

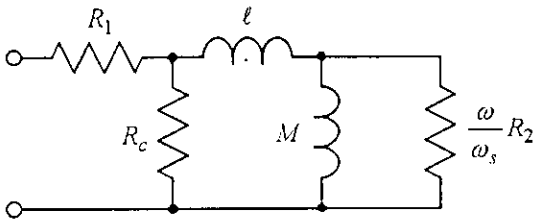

(c) Whole equivalent circuit of induction motor.

Fig. 3. Equivalent circuits of induction motor.

orientation. In the section, measurements of the motor parameters are briefly reviewed to clarify some assumptions in the following discussion [5]. The measurements are conducted according to three kinds of experimental tests as usual, dc excitation test, no load test, and lock test. The stator resistance is measured with ease by exciting the motor with a dc voltage source. When the no load test is conducted, several parameters are calculated according to the equivalent circuit shown in Fig. 3(a). In the figure, a resistance which equivalently acts as a dissipater of the core loss is connected in parallel with the stator inductance. The equivalent core loss resistance and the stator inductance can be calculated by the following process :

$$R_c = \frac{R'^2 + X'^2}{R'}, \text{ and} \tag{7a}$$

$$L_{11} = \frac{R'^2 + X'^2}{\omega X'}, \tag{7b}$$

where the intermediate parameters R' and X' are obtained by :

$$R' = \frac{P_0 - P_m}{3I_0^2} - R_1, \text{ and } X' = \sqrt{\frac{V_0^2}{3I_0^2} - \left(\frac{P_0 - P_m}{3I_0^2}\right)^2}.$$

In the above calculation, the motor variables and parameters are defined as follows :

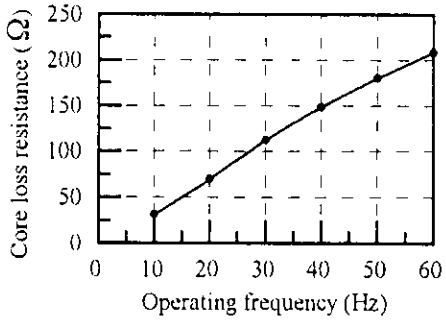

(a) Characteristic for test motor A.

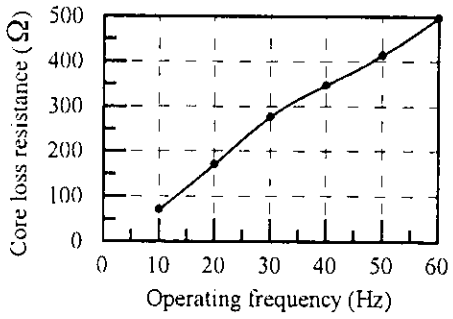

(b) Characteristic for test motor B.

Fig. 4. Characteristics of equivalent core loss resistance.

V_0 : stator terminal voltage (rms) at no load,

I_0 : stator line current (rms) at no load,

P_0 : dissipated power at no load,

P_m : mechanical power loss at no load,

ω : operating angular frequency,

R_1 : stator resistance,

R_c : equivalent core loss resistance, and

L_{11} : stator inductance.

The lock test is subsequently conducted on the basis of the equivalent circuit shown in Fig. 3(b). The rotor resistance, the magnetizing inductance and the leakage inductance are calculated by the following process :

$$R_2 = R''\left(\frac{R''^2 + X''^2}{X''^2}\right), \tag{8a}$$

$$M = \frac{X''}{\omega}\left(\frac{R''^2 + X''^2}{X''^2}\right), \text{ and} \tag{8b}$$

$$\ell = L_{11} - M, \tag{8c}$$

where R'' and X'' are obtained by :

$$R'' = \frac{P_s}{3I_s^2} - R_1, \text{ and } X'' = \omega L_{11} - \sqrt{\frac{V_s^2}{3I_s^2} - \left(\frac{P_s}{3I_s^2}\right)^2}.$$

The variables and the parameters are defined as follows :

V_s : stator terminal voltage (rms) with rotor locked,

I_s : stator line current (rms) with rotor locked,

P_s : dissipated power with rotor locked, and

R_2 : rotor resistance.

TABLE I SPECIFICATIONS OF TEST MOTORS

	Test Motor A	Test Motor B
Rated Power (kW)	1.5	1.5
Rated Torque (Nm)	8.63	10.1
Rated Voltage (V)	180	200
Rated Current (A)	8.1	6.8
Rated Frequency (Hz)	55	50
Rated Speed (rpm)	--	1420
Number of Poles	4	4

Consequently, the equivalent circuit of the induction motor on the whole can be drawn as shown in Fig. 3(c). It should be noted that the leakage inductance on the rotor side has been equivalently canceled out and automatically converted to the stator side when the calculation processes described above are taken.

Fig. 4 shows characteristics of the equivalent core loss resistance which have been measured on the basis of the method. Two kinds of induction motors of which specifications are shown in TABLE I have been tested. In order to make the measurements as accurate as possible, a precise VVVF analog power amplifier which is able to generate pure sinusoidal waveforms has been used. Although the value of the resistance is known to be proportional to the operating frequency to the 1.6 power, the results can be approximated as linear proportional functions of the operating frequency within the range of less than 60Hz. On the assumption, the equivalent core loss resistance is written as follows using a coefficient k_c :

$$R_c \approx k_c \omega . \tag{9}$$

B. Torque control performance without compensation

Fig. 5 shows a characteristic of the control error against the output torque obtained by computer simulations. In the simulations, a model of the test motor A in which the equivalent core loss resistance had been incorporated was employed as a controlled object (cf. Appendix). When the motor is controlled by the system shown in Fig. 1 and 2, which has not introduced the core loss compensation, the error raises up to 7% as the output torque increases. It can be found that the core loss brings not only insufficient output torque but also non-linearity in torque control. The output torque error should be avoided for the applications which require accurate pressure or tension control such as plastic forming or winding machinery. In what follows, a simplified method to overcome the problem is described.

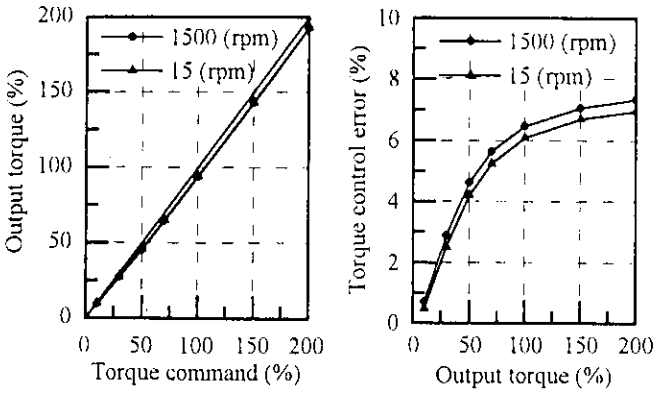

Fig. 5. Characteristic of torque control without core loss compensation.

IV. IMPROVED TORQUE CONTROL IN CONSIDERATION OF EQUIVALENT CORE LOSS RESISTANCE

A. Modified control system with core loss compensation

The direct field-oriented control system is inherently composed of two blocks, the feedforward block and the feedback block, as previously described. The feedforward block converts the torque and flux commands into the d-axis and q-axis current commands, while the feedback block estimates the rotor flux and performs the coordinate transformations to regulate the currents on the rotor flux ($d-q$) coordinates. Since both of the blocks include the motor model, the equivalent core loss resistance has to be considered for both.

In order to make the consideration simpler, it is assumed that the leakage inductance is much smaller than the magnetizing inductance and the influence of the leakage flux on the rotor circuit is negligibly small compared with the main flux in the steady-state equivalent circuit. On the assumption described here, the equivalent core loss resistance can be moved to another position which is in parallel with the magnetizing inductance in the circuit. Then it is possible to suppose that some amount of the q-axis current bypasses the equivalent core loss resistance, which probably causes insufficient torque current to the rotor circuit. Therefore, a current command which corresponds to the bypassing component should be superposed beforehand on the q-axis current command in (1). The current component i_c^* to be superposed for the core loss compensation is derived by simply dividing the steady-state induced voltage by the equivalent core loss

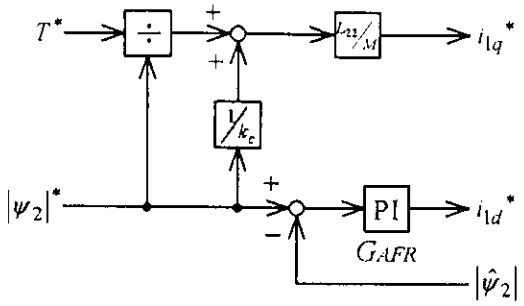

(a) Modified current command calculation block.

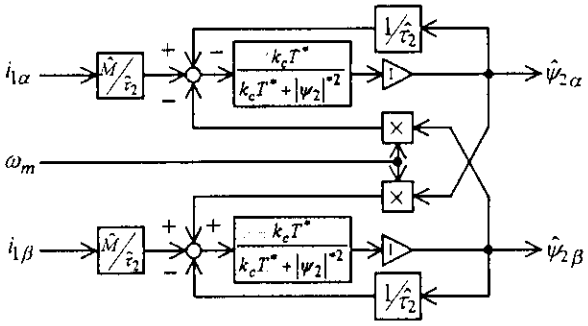

(b) Modified rotor flux simulator block.

Fig. 6. Modified field-oriented control blocks.

resistance on the rotor flux ($d-q$) coordinates as follows :

$$i_c^* = \frac{\omega \frac{L_{22}}{M}|\psi_2|^*}{R_c} = \frac{L_{22}}{M}\frac{|\psi_2|^*}{k_c}. \tag{10}$$

In the above derivation, the frequency characteristic of the equivalent core loss resistance described by (9) is utilized. Consequently, the modified q-axis current command can be obtained from (1) and (10) as :

$$i_{1q}^* = \frac{L_{22}}{M}\left(\frac{T^*}{|\psi_2|^*} + \frac{|\psi_2|^*}{k_c}\right). \tag{11}$$

It can be found that the above equation is identical with the q-axis current command in (1) when k_c is infinite. Since the equivalent core loss resistance diverges in case of the infinite k_c, this condition corresponds to the fact that no core loss has been assumed in the conventional field-oriented controller. The core loss compensation considered in the above discussion is performed on the rotor flux ($d-q$) coordinates with respect to a current amplitude. Unless the rotor flux is correctly estimated taking the core loss into consideration, the feedforward compensation on the coordinates must not be carried out properly. Therefore, it is necessary to investigate the core loss compensation for the feedback block, what is called the rotor flux simulator.

The rotor flux estimation error necessarily occurs in the simulator shown in Fig. 1(b) because of the model

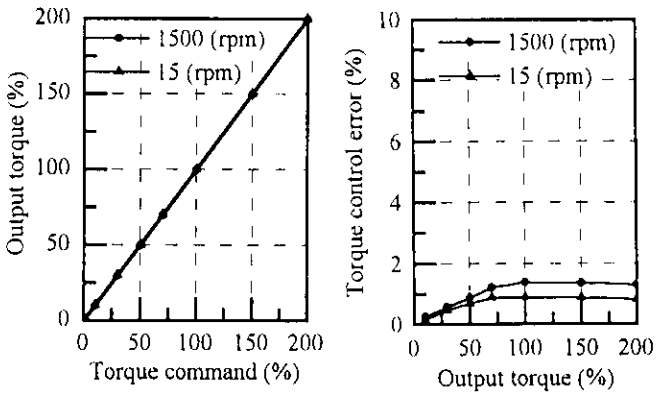

Fig. 7. Characteristic of torque control with core loss compensation.

mismatch owing to the equivalent core loss resistance. On the assumption that the equivalent core loss resistance is in parallel with the magnetizing inductance, it is considered that the resistance has influence on the rotor time constant in the simulator and the rotor time constant is changed by a ratio of $\left(i_{1q}^* + i_c^*\right)/i_{1q}^*$. Substituting i_{1q}^* of (1) and (10) into the ratio, the rotor flux simulator of (2) can be modified as follows :

$$\hat{\psi}_{2\alpha\beta} = \frac{\hat{M}}{1+(\mathrm{p}-\mathrm{j}\omega_m)\hat{\tau}_2\frac{i_{1q}^* + i_c^*}{i_{1q}^*}} i_{1\alpha\beta}$$

$$= \frac{\hat{M}}{1+(\mathrm{p}-\mathrm{j}\omega_m)\hat{\tau}_2\left(1+\frac{|\psi_2|^{*2}}{k_c T^*}\right)} i_{1\alpha\beta}. \tag{12}$$

This equation is identical with the rotor flux simulator of (2) when k_c is infinite as well as (11). Fig. 6 shows both modified blocks which correspond to (11) and (12), and only the coefficient k_c in (9) is necessary to compensate the core loss according to the figures, which can simplify the configuration of the whole control system.

By employing the modified rotor flux simulator represented by (12), the parameter identifier shown in Fig. 2 can be utilized without any modification of its configuration to estimate the motor parameters, because the core loss dose not have relation with the instantaneous reactive power.

B. Improved torque control performance

Some simulation tests have been conducted under the same condition as that of Fig. 5. in order to verify the

validity of the method. Fig. 7 shows the characteristic of the torque control error against the output torque. As shown in the figure, the error has been reduced down to less than 2%, and it is found that the error hardly increases even though the output torque is increased. It is supposed that the remaining error has been caused by a model mismatch owing to the position of the equivalent core loss resistance in the equivalent circuit. Also, in a strict sense, it should be considered that the resistance affects not only q-axis but also d-axis in the feedforward block, and the feedback block must be more complicated than what has been considered in the above discussion. However, it would be recognized that the method presented in the paper gives the direct field-oriented controller an effective and simple solution to compensate the torque control error caused by the core loss.

V. Conclusion

In the paper, a simplified precise torque control strategy of an induction motor has been described. The torque control system consists of two subsystems which should incorporate modification of the machine model by taking core loss into consideration. One is a direct field-oriented controller with a rotor flux simulator, which makes it possible to control the output torque and the rotor flux independently like a separately exited dc motor. The other is a robust parameter identifier utilizing instantaneous reactive power of the induction motor, which enables the system to compensate the parameter mismatch in the flux simulator with no sensitivity to the stator resistance. Owing to the model mismatch caused by the core loss in the motor, however, both the field orientation and the parameter identification cannot be carried out perfectly, which results in inaccurate torque control. The paper has presented a simple solution to improve the accuracy with small modifications of the feedforward and feedback blocks in the direct field-oriented controller. Consequently, quite precise torque control characteristic within 2% error has been verified through computer simulation tests, which shows possibility of reducing the output torque error effectively.

References

[1] T. Mizuno, J. Takayama, T. Ichioka, and M. Terashima, "Decoupling Control Method of Induction Motor Taking Stator Core Loss into Consideration," *IEE Japan Trans. Ind. App.* , vol. 109-D, No. 11, pp. 841-848, 1989.

[2] E. Levi, "Impact of Iron Loss on Behavior of Vector Controlled Induction Machines," *IEEE Trans. Ind. App.* , vol. 31, No. 6, pp. 1287-1296, 1995.

[3] M. Sokola, E. Levi, G. Jamieson, and D. Williams, "Representation and Compensation of Iron Loss in Rotor Flux Oriented Induction Machines," *1996 PEDES Conf. Rec. - New Delhi*, vol. 1, pp. 243-249.

[4] T. Noguchi, S. Kondo, and I. Takahashi, "Field-Oriented Control of an Induction Motor with Robust On-Line Tuning of Its Parameters," *IEEE Trans. Ind. App.* , vol. 33, No. 1, pp. 35-42, 1997.

[5] H. Nakano, H. Akagi, I. Takahashi, and A. Nabae, "A New Type Equivalent Circuit of a Induction Motor Based on the Total Linkage Flux of the Secondary Windings," *IEE Japan Trans. Power. Elec.* , vol. 103-B, No. 3, pp. 216-222, 1983.

Apendix

The induction motor which has been controlled in the computer simulations is based on the following model [1] :

$$\begin{bmatrix} v_{1dq} \\ 0 \end{bmatrix} = \begin{bmatrix} R_1 + R_m + \mathrm{p}L_{11} + \mathrm{j}\left(\omega L_{11} - \mathrm{p}\dfrac{R_m}{\omega}\right) & R_m + \mathrm{p}L_m + \mathrm{j}\left(\omega L_m - \mathrm{p}\dfrac{R_m}{\omega}\right) \\ \omega_s \dfrac{R_m}{\omega} + \mathrm{p}L_m + \mathrm{j}\left(\omega_s L_m - \mathrm{p}\dfrac{R_m}{\omega}\right) & R_2 + \omega_s \dfrac{R_m}{\omega} + \mathrm{p}L_{22} + \mathrm{j}\left(\omega_s L_{22} - \mathrm{p}\dfrac{R_m}{\omega}\right) \end{bmatrix} \begin{bmatrix} i_{1dq} \\ i_{2dq} \end{bmatrix},$$

where

$\omega_s = \omega - \omega_m$: slip angular frequency,

$R_m = \dfrac{\omega^2 M^2}{{R_c}^2 + \omega^2 M^2} R_c$: equivalent core loss resistance,

and

$L_m = \dfrac{{R_c}^2}{{R_c}^2 + \omega^2 M^2} M$: magnetizing inductance.

The resistance R_m is considered to be in series with the inductance L_m in the model described above.